Computational Fluid Dynamics Analysis and Optimization of a Savonius Vertical Axis Wind Turbine for De La Salle University Campus

Aristotle Ubando[1a], Antonio Maralit[2b], Kenneth Nyanasengeran[3c], Matthew Timothy Pua[3d], Maoi Marcelino[3e], Roberto Louie Moran[3f]*

[1]Center for Engineering and Sustainable Development Research (CESDR), De La Salle University, Manila, Philippines
[2]Sustainability Campus Office, De La Salle University, Manila, Philippines
[3]Student, Mechanical Engineering Department, De La Salle University, Manila, Philippines
*robert_moran@dlsu.edu.ph

Abstract: The Savonius design is one of the simplest wind turbines ever developed. It operates by taking advantage of the drag differentials of two air surfaces. Conceived by Finish engineer Sigurd Johannes Savonius in 1922, it has a distinct 'S' shape, with a concave surface catching or scooping the wind, a convex surface opposing it, and a small gap allowing the wind to pass from the catching air surface to the opposite air surface – although some configurations are made without that last feature. Our study focuses on the optimum dimensions for such a turbine extracting wind energy on Henry Sy lawn. We measured wind conditions in that area and found an average of 2.7 meters per second. We then considered three main dimensions, diameter, gap, and height of the turbine, as adjustable parameters we can experiment with in a Computational Fluid Dynamics simulator. A computerized fluid simulation study was constructed and run in ANSYS Fluent CFD simulator, coupled with a Direct Optimization tool on the ANSYS 14.5 workbench – both communicating with each other. The DO tool generated 150 configurations of the design, based on programed limits of the gap, radius, and height; simulated all these configurations in the Fluent CFD, and gave five best configurations. Of the five, the best dimensions for our simulated wind conditions were within the following values: 27.5 to 33 mm gap, 150 to 170 mm radius, and 1.2 to 1.4 meter height. Future work involves the testing validation of the actual Savonius vertical axis wind turbine at Henry Sy hall.

Keywords: VAWT; Wind Energy; Wind Turbine; Renewable Energy; CFD

1. INTRODUCTION

As governments, nations, and industries look to renewable energy to meet the ever the growing energy demand, energy production needs to increase in efficiency while decreasing negative environmental impact. Urban energy is one of the most demanding components of the human energy demand. According to the IEA, in 2012 the global production of electricity totaled 13,461.14 Mtoe (Million tons of oil equivalent world-wide) or approximately 157 GW-hours (International Energy Agency, 2014). Of that amount, 2,076.1 Mtoe of electricity (approximately 24 GW-hours) was consumed by urban and residential populations. Natural gas, oil, and coal made up 81.7% of the total

world energy share (excluding the electricity trade). Renewables such as hydro and biofuel gas got 2.4% and 10%, respectively, of the total energy share. Wind energy, along with geothermal and solar energy, has not gained the attention it deserves as useful energy source; Combined, these sources make-up only 1.1% of the total world's utilized energy. Regionally, wind energy got 1.1% of the total utilized energy share in the OECD nations of the Americas, 2.3% in the OECD nations of Europe, and 1.2% in the OECD nations of Asia and Oceania. However, the World Energy Outlook 2014 predicts that the global subsidies on renewable energy will reach $230 billion dollars in 2030 (International Energy Agency, 2014), because of policy changes regarding these. This all means more subsidies for research and production of wind turbines. The source predicts that subsidies on wind energy will peak in 2020, giving regions more

opportunity to increase its world and regional energy production share. The creation of urban wind turbines could change the situation of wind energy. Independent power stations harvesting wind may serve as an independent, or off the main electricity supply-grids, source of cheap, clean, and renewable energy.

WIND TURBINES

There are numerous types and designs of wind-turbines all of which can be classified into the type of interaction they exhibit between blade and wind flow (drag producing, lift producing, or both) and orientation of the axis. There are two types of axis orientation: Vertical Axis Wind Turbines or VAWT which are parallel to the ground and Horizontal Axis Wind Turbines or HAWT which are perpendicular to the ground. HAWTs are the most popular wind turbines in production to date and are well suited for large scale wind harvesting because devices boast generally large efficiencies and low starting speeds. However, the advantages VAWTs have over them are their ease of manufacturing, robust design, low tip-speed ratio, and fewer parts.
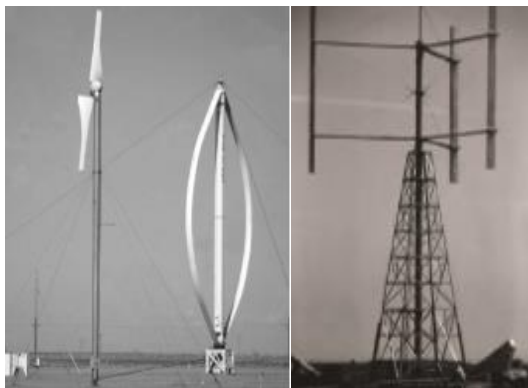

Fig. 1. Errected Giromill turbine, left, and Darrieus turbine, right. (Ghassemi & Nelson, 2011)
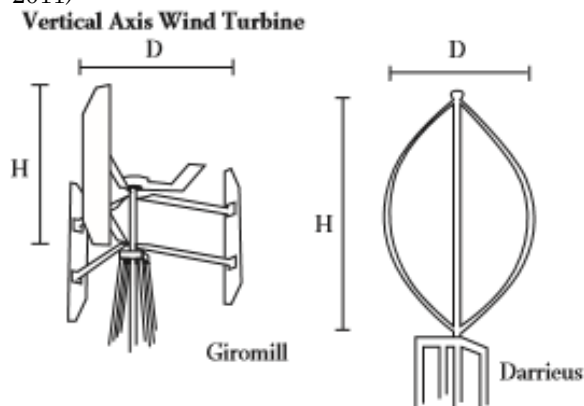

Fig. 2 Template designs of Giromill and Darrieus VAWT (Ghassemi & Nelson, 2011)

VAWT blades have the least complicated blade design among the two classes. Their blades can also be directly coupled to a gearbox, minimizing mechanical losses, assembly, and moving parts. They accept wind from any direction and speed, negating the need for a wind-vane or directional guide. Examples of Vertical Axis Wind Turbines aside from the Savonious are the Giromill and Darrieus shown in figures 1 and 2. The Darrieus is a lift-type turbine, constructed with two or three blades, vertically inclined in parabolic shapes which meets at the top and bottom. It uses a slim symmetrical airfoil, redirecting air behind the airfoil pushing the blade forward. The Giromill is another lift-type, with two airfoils constructed vertically strait this time. This also redirects air behind the blades, causing them to move forward and rotate the axis. Both have high
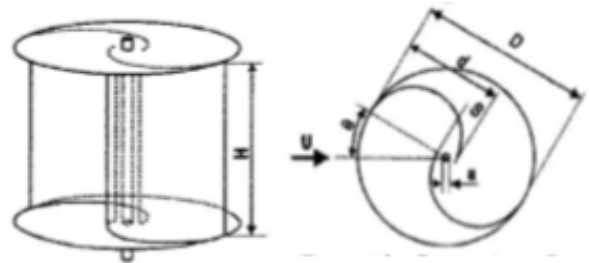

Fig. 3 Savonius design and dimensions (Ubando, Publico, & Paran, 2010)

starting speeds, so they would have to be modified with a starting motor.

The Savonius wind turbine is constructed with two or more simply shaped, scooping blades that catch the air from any direction, as shown in Figure 3. It has a concave and convex blade, with a small gap between the meeting tips. This gap can be positive, each blade's end-points inside the circumference and covering the gap, or negative, end-points outside the circumference and exposing the gap. The Savonius uses both drag and lift to generate rotation, by allowing the air to push the concave blade and then be redirected behind the convex blade. It has simple and straight-forward blade construction, even with a few modifications, and robustness of design. Depending on the design, a Savonious would have a low starting speed.

COMPUTATIONAL FLUID DYNAMICS

It is common practice to conduct aerodynamic performance tests for products like a turbine inside wind-tunnels. However, methods exist for purely numerical studies using Computational Fluid Dynamics or CFD simulators. They are sensitive to domain size (or the size of fluid/solid meshes in the simulator), turbulence models used, and the complexity developed by the air flow. These

SEE-II-015

2

can use 2 dimensional or 3 dimensional flow. Our study used a 3 dimensional flow, or fluid particles moving in 3 dimensions. A mesh is computer generated volume divided into triangles, cubes, or other volumes or areas that a computer could easily and numerically analyze. In the case of CFD, the mesh numerically represents air around the product or aerodynamic object under study, usually termed as the domain, while the product is a hollow shape cut-out within the mesh. These analyses are done with turbulence models, viscosity and density models, energy equations, and other models that quantify fluid behavior. The simulator will use CPU resources to calculate until equations converge, or values within each 3D volume or 2D area in a mesh agree with each other. Transient simulations, which were also conducted in this study, are simply multiple steady simulations, or time-steps, accepting changing parameters and using data from the
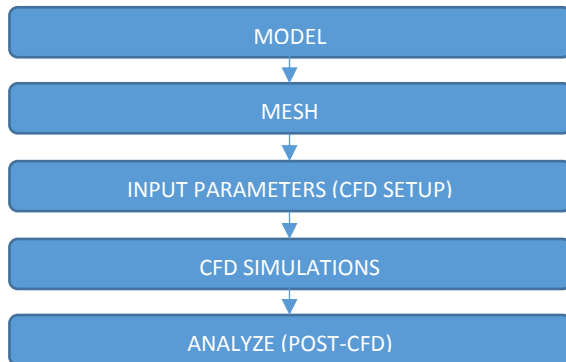

Fig. 4. Order of CFD processing and simulation in the ANSYS workbench

previous time-step. Processing these simulations start with modeling and meshing and end with actual simulating and post-processing, as shown in Figure 4:

Previous studies give us a better understanding of turbulence models in the Fluent software. There are nearly 24 turbulence models available in Fluent 14.5; the one used in this study is the RNG k-ε model developed by Yakhot and Smith in 1992 (Ubando, Publico, & Paran, 2010). This model computes variables of turbulent airflow (variables being x-y-z positions and parameter states) by considering turbulent kinetic energy of moving air particles, k, and the dissipation rate of the turbulence, ε (Fluent Inc., 2006). The standard k-ε model is able to predict developing thin layers and ducted flows in fully turbulent flows without changing model constants. Transport models for k and ε, taken from the Fluent 6.3 documentation, are shown in Eq. 1 and 2:

$$\frac{\partial \rho k}{\partial t} + \frac{\partial \rho k u_i}{\partial x_i} = \frac{\partial}{\partial x_j}\left(\alpha_k \mu_{eff} \frac{\partial k}{\partial x_j}\right) + G_k + G_b - \rho\varepsilon$$
$$- Y_M + S_k \quad \text{(Eq. 1)}$$

$$\frac{\partial \rho \varepsilon}{\partial t} + \frac{\partial \rho \varepsilon u_i}{\partial x_i} = \frac{\partial}{\partial x_j}\left(\alpha_k \mu_{eff} \frac{\partial \varepsilon}{\partial x_j}\right) + C_{1\varepsilon}\frac{\varepsilon}{k}G_k$$
$$- C_{2\varepsilon}\rho\frac{\varepsilon^2}{k} - R_\varepsilon + S_\varepsilon \quad \text{(Eq. 2)}$$

where:

ρ = fluid density

$a_{k \, or \, e}$ = Prandtle numbers for k and e transport models

μ_{eff} = effective viscosity evaluated by fluent

G_k = turbulent kinetic energy due to mean velocity gradients

Y_M = dissipation of turbulence due to fluctuating dilation in compressible fluid

$S_{k \, or \, \varepsilon}$ = user-defined inputs in source surfaces

$C_{1\varepsilon}$ = 1.42, constant given by RNG theory

$C_{2\varepsilon}$ = 1.68, constant given by RNG theory

R_ε = turbulence contributed by high Reynolds number flow, term given by RNG theory

The RNG k-ε model has an additional of a term, R_ε, in the ε-transport model, from the Renormalized Group Theory, to account for effects of lower Reynolds number on viscosity and rapid rate of strain and streamline curves. An additional modified model, Equation 3 and also found in the Fluent 6.3 documentation, accounts for swirl flows. It is still, however, sensitive to near-wall conditions.

$$\mu_t = \mu_{t0}f\left(\alpha_s, \Omega, \frac{k}{\varepsilon}\right) \quad \text{(Eq. 3)}$$

where:

μ_{t0} = value of unmodified viscosity model, $\rho C_\mu k^2/\varepsilon$

C_μ = 0.0845, derived by RNG

a_s = swirl constant

Ω = Characteristic swirl number evaluated in Fluent

CFD data with wind-tunnel data from Hayashi testing a simple Savonius turbine design is co-related to CFD by a past study that used ASNSY Fluent 12. (Ubando, Publico, & Paran, 2010). The purpose of this study was to find the best turbulence model that would agree with real world data for performance testing the Savonius turbine. The study manually simulated 36 steady simulations with different meshes at different angles of rotation, 5 degrees apart. It tested the 4 turbulence models and found that, among the four models, an RNG k-ε turbulence model showed the most correlation with real-world data. With this model, a large domain was

optimal, at least 10D for each lateral distance and 10H for the top and bottom domains. It also found that a coarse mesh domain, or a mesh cut into larger and fewer volumes, would take twice as simulation time (time it takes for a simulation to converge) as a fine domain, or a mesh cut into smaller and more numerous volumes, but would still be as accurate. Simulation time was found to be proportional to mesh quality and domain size.

A similar numerical study from Mansura University in Egypt (Gad, AbdEL-hamid, El-Askary, & Nasef, 2013) used the SST k-ω turbulence model to analyze the performance of a Savonius turbine with modified blade shapes. The standard k- ω this time considers kinetic energy, k, and the specific dissipation rate, ω. It is able predict separation of flow due to the pressure gradient, which is an advantage over k-ε models. The modified model, SST k-ω incorporates modifications for low Re number calculations and fluid compressibility. SST k-ω also uses k-ε transport models to predict fluid flows far from the walls, while using k-ω models to predict near-wall flow. The study also utilized a rotating mesh inside a larger rectangular domain, both finely meshed. This allows for a dynamic simulation with a rotating turbine. The separation of fixed and rotating mesh is shown in Figure 5. The blade shapes were created by fixing the end points of each blade and applying a moving loci of 8 points with an adjustable gap size to create different curves. The model was simulated in Fluent 6.3 and a total of 8 designs were tested, including different, unconventional V-shape designs and triangular shapes.
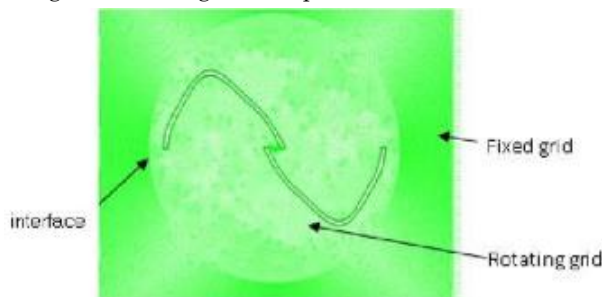

Fig. 5. Study by Gad, 2013, zoom in of rotating mesh

Aside from the turbulence models, three other equations were used in this study: the Energy Equation model and incompressible idea-gas density and Sutherland viscosity properties. These are all available in the Fluent 14.5 models and can be understood better, along with the turbulence models in the User-Help and Tutorials available online or with the software (Fluent Inc., 2006).

SCOPE OF THE STUDY

The objective of our study is to find an optimum design for a Savonius turbine that will extract wind energy at the Henry Sy Garden. Located at De La Salle University, an urban Savonius turbine would match the Henry Sy building's modern architecture and display the school's spirit of innovation. It was important the turbine also be visible for students, staff, and visitors of the campus. Wind speed tests were taken at the grounds of Henry Sy hall and the garden facing Taft Avenue. The area has wind speeds as high as 4 m/s but an average of 2.7 m/s was found. The study is limited to optimizing the design of a straight Savonius with a positive gap for that speed. Future study within the year will include design and fabrication of the turbine for actual use.

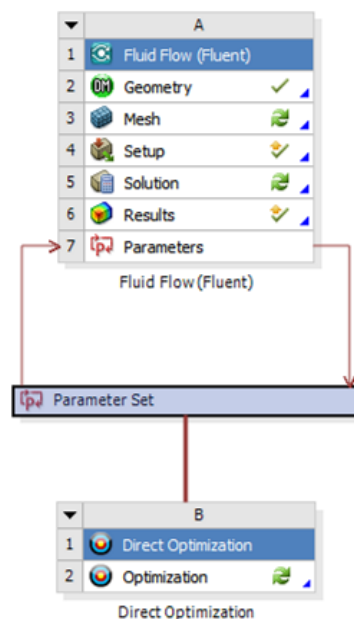## 2. PRE-PROCESSING

PARAMETERS

Fig. 6. 'Parameter Set' section couples Fluent component and DO. Parameters can be thrown to or from any component

The Savonius depends on a force differential between the two blades in favor of the leading blade and moment force, both causing rotation. Both the push of air on the leading concave shape and the redirection of air into the gap then to the secondary concave blade creates drag force and moment torque to actuate rotation. The most important user-input parameters or dimensions in the simplest design would be:

(1)   Turbine Height
(2)   Cup radius (both cups being equal in

radius)
(3)   Gap size (positive gap)

The output parameters of the optimization study are the moment and drag forces developed on the surfaces of the turbine. All these inputs and outputs are set apart and handled by the 'Parameter Set' section, as shown in Figure 6. Once a parameter is inside the set, their values can be changed by user input or a Design Expert tool.
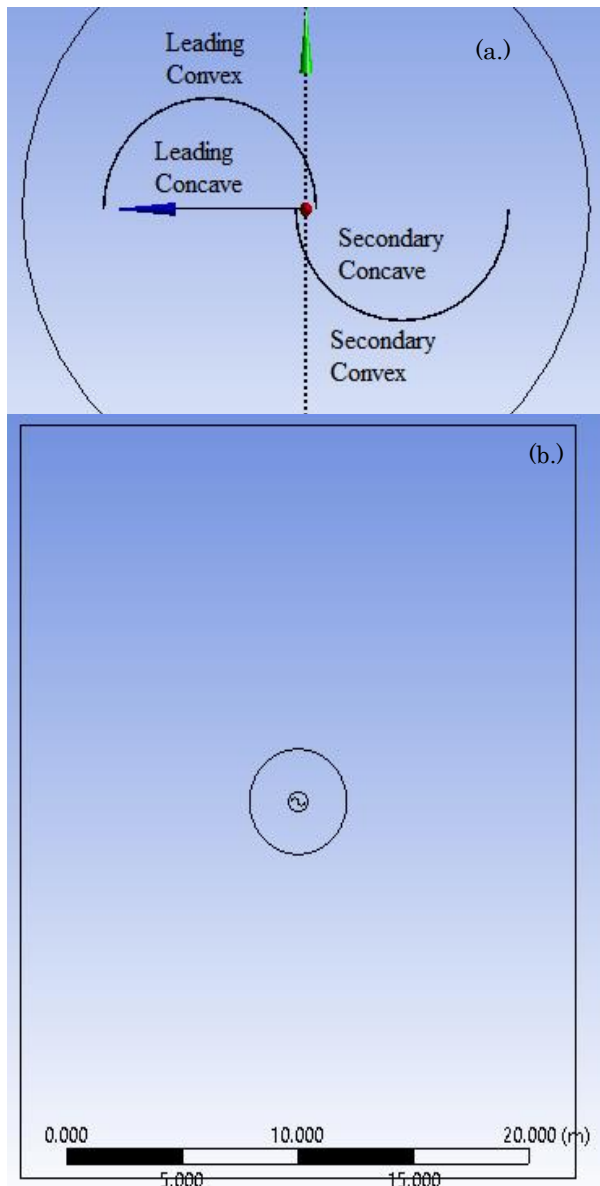
MESH MODEL

Fig. 7. (a) Surface assignment of blades and large domains. (b) Large rectangular mesh; up is upwind and down is downwind surfaces

As shown in Figure 8, the model is a set of extruded cut-out at the center of a small, cylindrical domain 4.2 meters in diameter. It is bounded by a larger mesh shown in Figure 7b with 30 by 24 square-meter area. The top and bottom surfaces of both domains are parallel and 5 meters from the top and bottom of the turbine. The parameters are assigned Design Modeler and thrown to the Parameter Set. The Mesh Modeler generated a fine mesh with a relevance value of 60% for rougher calculations. A mesh with a higher relevance value of 100% and addition of a first level refinement method was used for refined calculations. The resulting statistics of both domains for 100% relevance were: 230,026 to 236,000 Nodes and 608,430 to 643,700 Elements. The resulting statistics of the rougher mesh, on average, were: 156,265 Nodes and 421,569 elements. Use of rough and fine calculations are explained in the methodology. Surface assignment was done on the Mesh Modeler tool, as shown in Figure 7a. These are simply arbitrary tags or IDs that Fluent and Parameter Set can call on later in the procedure as boundary zones.
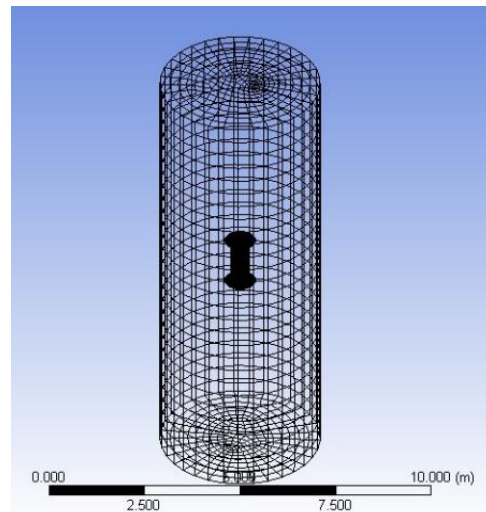

Fig. 8. Meshed model of smaller domain

FLUENT SETTINGS

In the software, number of processors for parallel computing and MPI connection types can be set with the software launcher. In the computer used for the study, shared memory, Intel-type MPI connection was used, set to 4 processes and double precision – making full use of the i5 core. The RNG k-epsilon was utilized in this study, with default coefficients and the Energy Equation.

Boundary zones, which were assigned during mesh modeling, can be set to certain boundary zones, interface settings, or surface monitors. A velocity inlet is assigned at the upwind

surface, where air will flow-speed of 2.7 m/s at STP (standard temperature and pressure, 288.16 °K and 101.325 kPa). Operating conditions were also set at STP. An outflow is assigned at the downwind surface, where air will simply exit the simulation. A Fluid Mesh Interface is assigned to the walls in the larger and smaller meshes that are touching each other. The smaller mesh and these walls are stationary during rough calculations. During refined calculations, the smaller mesh is assigned as a rotating mesh, about the y-axis and at 0.2618 rad/s ($15°\ s^{-1}$). An FMI will make sure fluid will "pass" through the boundary and not be treated as a wall. In other words, the simulator will try as best to analyze fluid passing through the boundary between the smaller and bigger domains as if it were not there.

Coefficients of moment and drag are taken from monitors assigned at the convex and concave surfaces of each blades. C_m monitors are combined (both convex and concave) for each blade while C_d monitors are assigned for each surface, individually. The viscus eddy forces on the convex-leading and the concave-secondary have little effect on the overall rotation. These monitors are thrown into the Parameter Set as output variables.

3. METHODOLOGY

OPTOMIZATION

During optimization, several samples were simulated successively, using the rough calculations explained in the previous section. Generated mesh with a relevance value of 60% was utilized in this procedure along with the following Fluent settings:

(1) Deactivated Double Precision
(2) Steady-state solution
(3) Constant density and viscosity for air material
(4) First order flow for all solution methods and SIMPLE pressure-velocity coupling
(5) Maximum iterations set to 14

This procedure made use of the Direct Optimization or DO, which directly optimizes a design based on user-input. The DO is able to control the input to generate samples, simulate within Fluent, and collect outputted data. It is able to do this through the Parameter Set and the thrown variables. The samples are random combinations of the values of the dimensional parameters, within upper and lower limits. The inputted range used in this study are as shown in Table 1:

Table 1. Height, width, radius range chosen from previous works

Lower Limit (mm)	Parameter	Upper Limit (mm)
120	Radius	350
500	Height	1200
9	Gap	35

The DO tool was set to generate 50 samples, choose 2 candidates, and 1 retry for each sample within 2 minutes. Equations 4 and 5 were inputted in the Parameter Set to analyze total moment force and force differential between the blades from outputs given by the surface monitors in the DO tool:

$$C_{m-Total} = C_{m-leading} + C_{m-secndary} \qquad \text{(Eq. 4)}$$
$$\Delta C_d = \left(C_{d-concave-leading} - C_{d-convex-leading} \right) - \left(C_{d-convex-second} - C_{d-concave-second} \right) \qquad \text{(Eq. 5)}$$

where:

C_m = coefficient of moment for assigned surface

C_d = coefficient of drag for assigned surface

ΔC_d = Force differential between blades or total drag force

Leading/Secondary - the blade monitored

Convex/Concave - the specific surface monitored

Two simple criterion were used: (1) largest resulting Total Cm, and (2) greatest force differential, ΔCd. Program was then executed within the DO, and all 50 samples were drawn, meshed, and simulated successively and resulting data was tabulated. The output here is the two candidate points based on the criteria set and following extracted data:

(1) Range of dimensional parameters: radius, height, and gap-size
(2) Performance range of two candidates
(3) Sensitivities and Trade-offs as analyzed by the DO

CHARACTERIZATION

During characterization, finer calculations are performed on the two candidate models with as much time as needed. Performance testing has to produce the most accurate results possible with as much time needed to validate the choice of design made by the DO tool and asses the performance of the new design. The following mesh settings are now used:

(1) Fine mesh with 100% relevance value
(2) 1st level refinement

Also, the Fluent settings are modified as so:

(1) Activated Double Precision
(2) Transient Solution
(3) Sutherland viscosity and incompressible, ideal-gas air density
(4) Rotating mesh (0.2618 rad/s or 15° s^{-1})
(5) All solution methods set to second order upwind flow.

Solution activities within Fluent are set to 12 time-steps per time-step size of 1 second and a maximum iteration number of 200 for each time step. A time-step size of 1 second tells Fluent to only adjust dynamic variables on a per 1-second basis. Rotation is the only dynamic variable in this procedure and, with those settings, 1 time-step will correspond to 15° angle. Data of dimensional parameters of the two candidates were exported from the DO tool to the Parameters Set so the entire project could be simulated and controlled from here. The output here is simulation data that can be analyzed using the Post-CFD tool. Using the Post-CFD tool, the following data was generated and tabulated in Excel:
(1) Refined Performance Range
(2) Total torque per time-step
(3) Drag force differential per time-step
(4) Velocity contours with streamlines

Moment and drag force coefficients are calculated from results of Fluent 14.5 using equations 6 and 7, taken from the Fundamentals of Aerodynamics (Anderson, 2001):

$$Total\ C_m = \frac{T}{\rho V^2 H w_t \cos(\theta)} \qquad (Eq.\ 6)$$

$$\Delta C_d = \frac{F}{\rho V^2 H w_t \cos(\theta)} \qquad (Eq.\ 7)$$

where:

ρ = fluid density, 1.225 kg/m^3
V = fluid velocity, 2.7 m/s
H = turbine height
w_t = width created by both cup, evaluated as $4Radius - 2Gap$-size
θ = instantaneous angle of rotation
F = instantaneous drag force, evaluated by fluent
T = instantaneous torque, evaluated by fluent

4. RESULTS AND DISCUSSION

OPTIMIZATION

The optimization study on 50 different samples and using the RNG k-ε model gives us two candidate points (or two best designs) which narrows the dimensional range as shown in table 2. These two

points also create performance range as shown in Figure 9. These are values reported in the surface monitors and they give us a good prediction of torque and moment values when the Savonius design is within the dimensional range. These values are at 0 degrees.
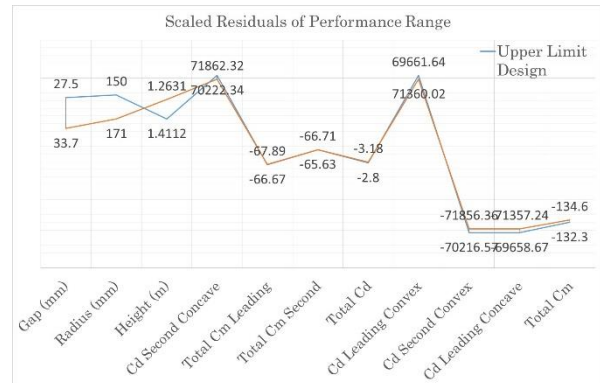

Figure 9. Performance range. Positions are scaled residuals while called out data are absolute values of dimensions and dimensionless coefficients
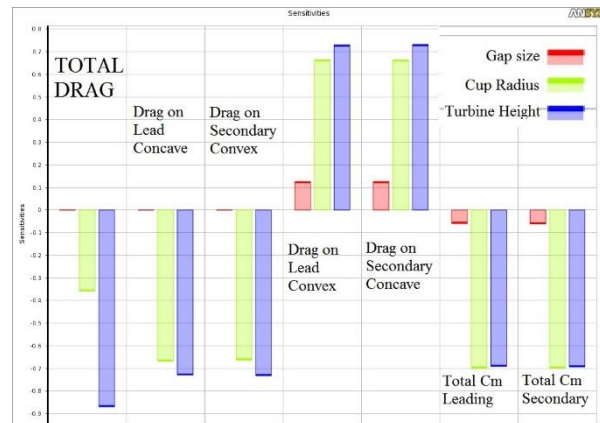

Figure 10. Percentage measurement of the output parameters' sensitivity to each dimensional parameter
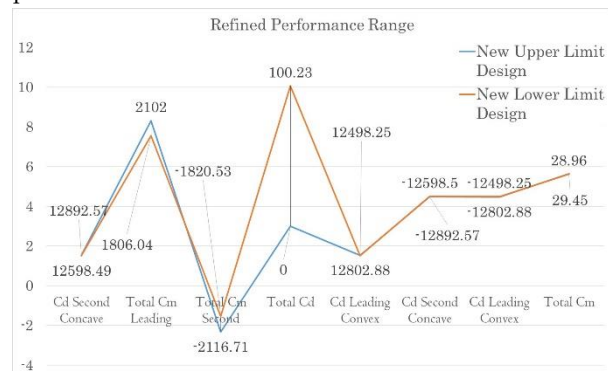

Figure 11. Refined Performance Range

Table 2. Resulting design range

Lower Limit (mm)	Parameter	Upper Limit (mm)
150	Radius	171
1263	Height	1411
27.5	Gap	33.75

This data was all extracted from the Direct Optimization tool. Not only does the DO give out these ranges, but it also analyze sensitivities in the design as shown in Figures 10.
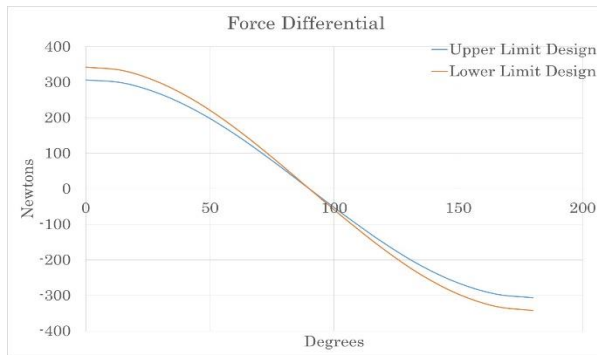

Figure 12. Drag force differential comparison of upper and lower limit design

CHARACTERIZATION

Both upper-limit and lower-limit designs were simulated and analyzed to validate and refine the performance range formulated. That is, two designs with radius, height, and gap of the specified lower and upper values in a transient simulation, using refined settings. A refined performance range was generated as shown in Figure 11, by calculating coefficients of drag and moment from values at 0 degrees to be able to compare it with the first
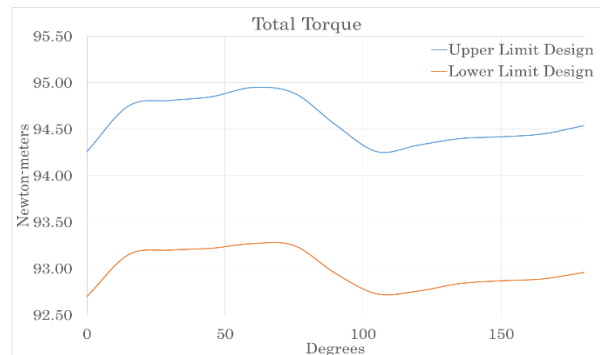

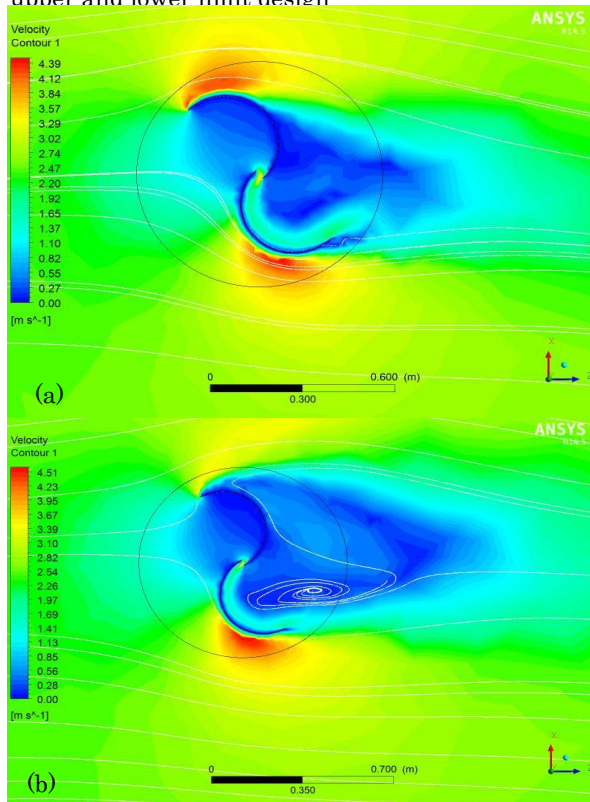Figure 13. Total moment force comparison of upper and lower limit design

(a)

(b)

Figure 14. Velocity contours and stream lines at 90 degrees. Leading blade becomes second and vice-versa.
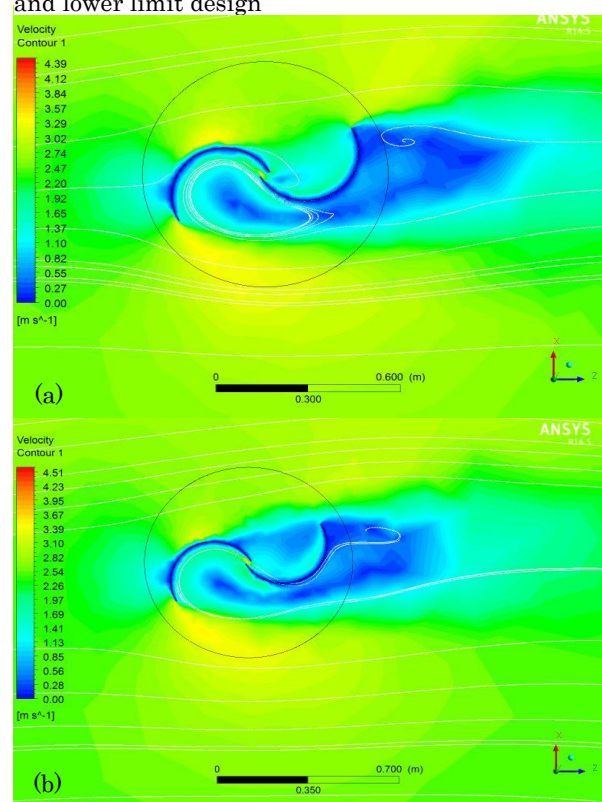

(a)

(b)

Figure 15. Velocity contours and stream lines of (a) upper range design and (b) lower range design, at 15 degrees. Blades are spinning against flow.

performance range. It shows that values have shifted in the graph. However, lower and upper ranges are still close together, save for Total Cd – the drag force differential.

Analyzing results from Post-CFD, two graphs were created to compare drag force differential and total moment force of each design, per angle. These are shown in figures 12 and 13. Contours of velocity with stream-line patterns were also extracted from the Post-CFD for 3 different angles, as shown in the sets of images in figures 14 and 15.

5. CONCLUSIONS

Table 2 and Figure 11, gives us the best performance within a narrow range of dimensions of a Savonius turbine design. This, however, is under the most ideal conditions and specifically for the specified wind-speed, set at 2.7 m/s. These calculations also do not take into account weight of material or load on turbine. The large difference in drag force differential, shown in Figure 11, may be due to the difference in height, as analyzed by the optimization study in the sensitivities and shown in figure 10.

Plots of drag force difference, total moment force, and velocity contours help us characterize the performance of both optimized designs. The upper-limit design seems to generate more torque per angle, as seen in Figure 4.6; however, values from figures 4.5 and 4.6 show that measured performance isn't very far apart between the two designs. One critical feature is the use of the gap to recover kinetic energy of the air pushing the leading blade and feeding it to the secondary blade.

The gap size within 27.5 and 33.75 mm should accept the best amount of flow to produce the most moment force and differential drag-force, this is shown in figures 14 and 15. At 15 degrees; the larger gap size lets more in, allowing fast air to push the secondary blade, and reduces the wake-size of slow air, reducing drag at the secondary blade that would oppose rotation. Meanwhile at 90 degrees; the blade starts its transition. A design with a smaller gap does a better job of freeing air, reducing drag that opposes rotation. However, at this angle, a design with a larger gap allows faster air to come in the leading blade.

6. ACKNOWLEDGMENTS

The authors would like to acknowledge the Campus Sustainability Office and Campus Services Office of De La Salle University for forming the Green Swirl Team and handling the administrative processes necessary for this project and the Office of the Vice Chancellor for Research and Innovation and the University Research Coordination Office of the school for their assistance and consultation. Last but not the least, the team would like to bring honor back to God, without whom its members would not have the strength to carry out this research initiative.

7. REFERENCES

Anderson, J. D. (2001). Aerodynamic Force and Moments. In J. J. Anderson, *Fundementals of Aerodynamics* (pp. 19-20). New York: McGraw-Hill.

ANSYS, Inc. (2009, November). Design Exploration. Canonsburg, Pennsylvania, United States of America.

CFD Online. (2010, June 5). *RNG k-epsilon model*. Retrieved from CFD Online: http://www.cfd-online.com/Wiki/RNG_k-epsilon_model

Fluent Inc. (2006, 9 20). *FLUENT 6.3 User's Guide - 12.4.2 RNG k-ε Model*. Retrieved from FLUENT 6.3 Documentation: http://aerojet.engr.ucdavis.edu/fluenthelp/html/ug/node479.htm

Gad, H. E., AbdEL-hamid, A. A., El-Askary, W. A., & Nasef, M. H. (2013). Modification Of Construction Design Of Savonius Wind Turbine. *Eleventh International Conference of Fluid Dynamics*. Egypt: Mansura University.

International Energy Agency. (2014). IEA - Statistics. Paris, Cedex, France. Retrieved from IEA - International Energy Agency: http://www.iea.org/publications/freepublications/publication/key-world-energy-statistics-2014.html

International Energy Agency. (2014). *World Energy Outlook 2014 Factsheet*. Paris: IEA.

Nelson, V., & Ghassemi, A. (2011). Wind Energy. In *Introduction to Renewable Energy* (pp. 174-192). New York: CRC Press.

REUK Blog. (2015, January 18). *Darrieus Wind Turbines*. Retrieved from Renewable Energy Website: http://www.reuk.co.uk/Darrieus-Wind-Turbines.htm

REUK Blog. (2015, January 18). *Giromill Darrieus Wind Turbines*. Retrieved from The Renewable Energy Website: http://www.reuk.co.uk/Giromill-Darrieus-Wind-Turbines.htm

Ubando, A. T., Publico, A. S., & Paran, A. P. (2010). Turbulence Model Selection in Evaluating the Performance of Vertical-Axis Wind Turbine. *Regional Conference on Mechanical and Aerospace Technology* (pp. 97-103). Bali: University of the Philippines.